Seismic modeling using the frozen Gaussian approximation

Xu Yang, University of California Santa Barbara, Jianfeng Lu, Duke University, and Sergey Fomel, University of Texas at Austin

SUMMARY

We adopt the frozen Gaussian approximation (FGA) for modeling seismic waves. The method belongs to the category of ray-based beam methods. It decomposes seismic wavefield into a set of Gaussian functions and propagates these Gaussian functions along appropriate ray paths. As opposed to the classic Gaussian-beam method, FGA keeps the Gaussians *frozen* (at a fixed width) during the propagation process and adjusts their amplitudes to produce an accurate approximation after summation. We perform the initial decomposition of seismic data using a fast version of the Fourier-Bros-Iagolnitzer (FBI) transform and propagate the frozen Gaussian beams numerically using ray tracing. A test using a smoothed Marmousi model confirms the validity of FGA for accurate modeling of seismic wavefields.

INTRODUCTION

Ray theory (Cerveny, 2001; Popov, 2002; Engquist and Runborg, 2003) is a widely used approach to seismic modeling and migration. In this approach, one decomposes the wavefields into elementary waveforms that propagate along rays, and then constructs Green's functions or wavefields according to the dynamic information on rays (e.g. path trajectory, amplitude and phase). Kirchhoff migration (Gray, 1986; Keho and Beydoun, 1988) and Gaussian beam migration (Hill, 1990, 2001; Nowack et al., 2003; Gray, 2005; Gray and Bleistein, 2009; Popov et al., 2010) are the most famous seismic applications of this principle.

Dynamic ray tracing used in Kirchhoff migration is an effective method, however it produces unbounded amplitudes at caustics. The Gaussian beam approximation (GBA) retains the merits of ray tracing but can also handle multipathing while maintaining accuracy at caustics. However, in order to obtain a good resolution in GBA, one needs to tune the width parameter of Gaussian beams, especially because beams spread significantly in the process of wave propagation (Cerveny et al., 1982; Hill, 1990; Fomel and Tanushev, 2009). This parameter tuning becomes difficult in practical applications because of the heterogeneity of the media and the non-linearity of the Riccati equation involved in the beam construction. GBA relies on a Taylor expansion around the central ray, hence the error of the approximation increases when the beams become wider. Qian and Ying (2010) and Lu and Yang (2011) analyzed this phenomenon and showed that, even in the case of a simple velocity distribution, the error of GBA may grow rapidly in time.

In this paper, we adopt the frozen Gaussian approximation (FGA) method for computing seismic wave propagation in complex structures. The method was introduced in previous studies on general linear strictly hyperbolic systems (Lu and Yang, 2011, 2012a,b) and was originally motivated by Herman-Kluk propagator for solving the Schrödinger equation in quantum chemistry (Herman and Kluk, 1984; Kay, 1994, 2006). The main idea of FGA is to use Gaussian functions with fixed widths to approximate the propagation of seismic wavefields. These Gaussian functions are also known under the name *coherent states* in quantum mechanics, and mathematically form a tight frame in L^2-function space. The coherent state method was previously applied in seismic imaging (Albertin et al., 2001; Foster et al., 2002) but lacked the rigorous treatment of amplitude factors provided by FGA. Despite its superficial similarity with GBA, FGA is different at a fundamental level: In GBA, on the other hand, each Gaussian beam provides an approximate solution to the wave equation, which requires its width to change in time (Bleistein and Gray, 2010). In FGA, Gaussian functions are used only as building blocks for wave propagation. Each individual frozen Gaussian does not approximate a solution to the wave equation. Compared with GBA, FGA is able to provide a more accurate and robust solution due to the error cancellation phenomenon, especially in the situation of wave spreading (Lu and Yang, 2011, 2012a).

The main procedure of FGA is the following. The initial data are decomposed into a set of Gaussians with fixed predefined narrow widths. Each Gaussian function is then propagated along geometric rays. The amplitudes of the Gaussians are adjusted according to rigorously-derived dynamic equations so that, at the final time, the sum of them yields an accurate approximation to seismic wavefields or Green's functions. The basic ingredients of the FGA implementation are similar to those used in other ray-type or beam methods.

To accelerate numerical computation, we develop an algorithm for a fast Fourier-Bros-Iagolnitzer (FBI) transform algorithm (Folland, 1989; Martinez, 2002) to decompose the initial wavefields into Gaussians. The idea of decomposing functions into Gaussians is known in signal processing applications as *Gabor expansion* (Gabor, 1946; Helstrom, 1966; Bastiaans, 1980; Ma and Margrave, 2008). Thresholding criteria of initial Gaussian packets can be chosen to provide different levels of details depending on accuracy requirements and computational cost constraints.

THEORY

For simplicity, we shall consider wave propagation governed by the acoustic wave equation in d dimensions. The seismic wavefield u^ε is a function of time t and spatial variable $x \in \mathbb{R}^d$,

$$\partial_t^2 u^\varepsilon - c^2(x)\Delta u^\varepsilon = 0, \tag{1}$$

with initial conditions

$$u^\varepsilon(0,x) = f_0^\varepsilon(x), \tag{2}$$

$$\partial_t u^\varepsilon(0,x) = f_1^\varepsilon(x), \tag{3}$$

where $c(x)$ is the seismic velocity, and ε indicates the dependence on the (rescaled) wave length. We assume that $\varepsilon \ll 1$ is the high-frequency wave regime corresponding to short wavelengths.

FGA Formulation

FGA is an asymptotic-based approach to high-frequency wave propagation. Its complete derivation, error estimates (including validity at caustics), and generalization to other strictly hyperbolic systems are provided by Lu and Yang (2011, 2012a,b).

FGA gives the asymptotic approximation to the solution of equation (1) as a sum of Gaussian functions with fixed width,

$$\begin{aligned} u^{\varepsilon}_{\mathrm{FGA}}(t,x) = &\sum_{(q,p)\in G_+} \frac{a_+ \psi^{\varepsilon}_+}{(2\pi\varepsilon)^{3d/2}} e^{\frac{\mathrm{i}}{\varepsilon}P_+\cdot(x-Q_+)-\frac{1}{2\varepsilon}|x-Q_+|^2} \\ &+ \sum_{(q,p)\in G_-} \frac{a_- \psi^{\varepsilon}_-}{(2\pi\varepsilon)^{3d/2}} e^{\frac{\mathrm{i}}{\varepsilon}P_-\cdot(x-Q_-)-\frac{1}{2\varepsilon}|x-Q_-|^2}, \end{aligned} \tag{4}$$

where

$$\psi^{\varepsilon}_{\pm}(q,p) = \int_{\mathbb{R}^d} u^{\varepsilon}_{\pm,0}(y,q,p) e^{-\frac{\mathrm{i}}{\varepsilon}p\cdot(y-q)-\frac{1}{2\varepsilon}|y-q|^2}\,\mathrm{d}y, \tag{5}$$

$$u^{\varepsilon}_{\pm,0}(y,q,p) = \frac{1}{2}\Big(f^{\varepsilon}_0(y) \pm \frac{\mathrm{i}\varepsilon}{c(q)|p|} f^{\varepsilon}_1(y)\Big). \tag{6}$$

In equation (4), $\mathrm{i} = \sqrt{-1}$ is the imaginary unit, and "$+$" and "$-$" indicate the two wave branches, and $G_{\pm}$ are the sets of (q,p) pairs. Equation (5) is in a form of FBI transform (Martinez, 2002). In FGA, associated with each frozen Gaussian, the *time-dependent* quantities are: the center $Q_{\pm}$, momentum $P_{\pm}$ and amplitude $a_{\pm}$. The weight function $\psi_{\pm}$ is time-independent and computed initially, while the width of the Gaussian function is fixed at all times.

The evolution of $Q_{\pm}(t,q,p)$ and $P_{\pm}(t,q,p)$ satisfies the ray tracing equations corresponding to the Hamiltonian

$$H_{\pm} = \pm c(Q_{\pm})|P_{\pm}|\,. \tag{7}$$

For ease of notations, we will suppress the subscripts "$\pm$" when no confusion might occur. Hence (Q,P) solves

$$\begin{cases} \dfrac{\mathrm{d}Q}{\mathrm{d}t} = \partial_P H, \\ \dfrac{\mathrm{d}P}{\mathrm{d}t} = -\partial_Q H, \end{cases} \tag{8}$$

with initial conditions

$$Q(0,q,p) = q \quad \text{and} \quad P(0,q,p) = p. \tag{9}$$

The evolution of the amplitude $a(t,q,p)$ is given by

$$\frac{\mathrm{d}a}{\mathrm{d}t} = a\frac{\partial_P H\cdot\partial_Q H}{H} + \frac{a}{2}\,\mathrm{tr}\left(Z^{-1}\frac{\mathrm{d}Z}{\mathrm{d}t}\right). \tag{10}$$

with initial condition $a(0,q,p) = 2^{d/2}$. In (10), we have used the shorthand notations

$$\partial_z = \partial_q - \mathrm{i}\partial_p, \qquad Z = \partial_z(Q+\mathrm{i}P). \tag{11}$$

Here $\partial_z Q$ and $\partial_z P$ are understood as matrices, with the (j,k) component of a matrix $\partial_z Q$ given by $\partial_{z_j} Q_k$. The matrices $\partial_z Q$ and $\partial_z P$ can be solved at each time step by either divided difference or the following dynamic ray tracing equations,

$$\frac{\mathrm{d}(\partial_z Q)}{\mathrm{d}t} = \partial_z Q\frac{\partial^2 H}{\partial Q\partial P} + \partial_z P\frac{\partial^2 H}{\partial P^2}, \tag{12}$$

$$\frac{\mathrm{d}(\partial_z P)}{\mathrm{d}t} = -\partial_z Q\frac{\partial^2 H}{\partial Q^2} - \partial_z P\frac{\partial^2 H}{\partial P\partial Q}. \tag{13}$$

Componentwise, (12)-(13) can be written as (with Einstein's index summation convention)

$$\frac{\mathrm{d}(\partial_z Q)_{jk}}{\mathrm{d}t} = \partial_{z_j} Q_l\frac{\partial^2 H}{\partial Q_l\partial P_k} + \partial_{z_j} P_l\frac{\partial^2 H}{\partial P_l P_k},$$

$$\frac{\mathrm{d}(\partial_z P)_{jk}}{\mathrm{d}t} = -\partial_{z_j} Q_l\frac{\partial^2 H}{\partial Q_l Q_k} - \partial_{z_j} P_l\frac{\partial^2 H}{\partial P_l\partial Q_k}.$$

We need to point out a key difference here: In FGA, the solution of dynamic ray tracing equations (12-13) only affects the amplitude a, while in GBA, it affects both the amplitude and the beam width. We also note that equation (10) actually gives a conserved quantity along the Hamiltonian flow (8),

$$\frac{a^2}{c^2(Q)\det Z} = \text{constant}, \tag{14}$$

which implies that

$$a = \frac{c(Q)}{c(q)}(\det Z)^{1/2}, \tag{15}$$

with the appropriate branch of the square root continuously determined in time.

Initial wavefield decomposition

In order to apply representation (4) in practice, it is necessary to decompose the initial wavefield (2)-(3) into a sum of Gaussian functions, *i.e.* , to choose proper sets $G_{\pm}$ of (q,p) pairs in equation (4) and compute $\psi^{\varepsilon}_{\pm}$ in equation (5) correspondingly. Here we propose a local fast FBI transform to efficiently compute $\psi^{\varepsilon}_{\pm}$.

Let us rewrite equation (5) in the form

$$\psi^{\varepsilon}_j(q,p) = \int_{\mathbb{R}^d} f^{\varepsilon}_j(y) e^{-\frac{\mathrm{i}}{\varepsilon}p\cdot(y-q)-\frac{1}{2\varepsilon}|y-q|^2}\,\mathrm{d}y, \tag{16}$$

for $j = 0, 1$. Equivalently,

$$\psi^{\varepsilon}_j(q,p) = \int_{\mathbb{R}^d} f^{\varepsilon}_j(q+r) e^{-\frac{\mathrm{i}}{\varepsilon}p\cdot r-\frac{1}{2\varepsilon}|r|^2}\,\mathrm{d}r, \tag{17}$$

where we use the change of variable $r = y - q$. Define

$$g^{\varepsilon}_{q,j}(r) = f^{\varepsilon}_j(q+r)\exp(-\tfrac{1}{2\varepsilon}|r|^2), \tag{18}$$

then ψ^{ε}_j is given by the (rescaled) Fourier transform of $g^{\varepsilon}_{q,j}$,

$$\psi^{\varepsilon}_j(q,p) = \widehat{g^{\varepsilon}_{q,j}}(p/\varepsilon). \tag{19}$$

Notice that $g^{\varepsilon}_{q,j}$ contains an exponential function, hence its function value is negligible outside a localized domain centered around zero, for example, a small box

$$B_{\varepsilon} = [-L/2, L/2]^d \subset \mathbb{R}^d$$

with the length L scaled as $\mathcal{O}(\sqrt{\varepsilon})$. Therefore, $\psi_j^\varepsilon(q,p)$ can be evaluated efficiently by applying Fast Fourier Transform of $g_{q,j}^\varepsilon$ restricted on the small box B_ε.

Once $\psi_\pm^\varepsilon$ is computed, one can apply a simple thresholding to select the sets $G_\pm$ where $\psi_\pm^\varepsilon$ have relatively large values.

Algorithm

In summary, the FGA algorithm consists of three steps:

1. Initial decomposition: Choose the sets $G_\pm$ of (q,p) pair and calculate $\psi_\pm^\varepsilon$ defined in equation (5) from f_0^ε and f_1^ε;
2. Time propagation: Numerically integrate (8) and (10) up to the final time T;
3. Reconstruction: Compute the wave field at time T by applying equation (4).

With the modifications proposed by Tanushev et al. (2011), it is possible to generate initial data for Step 1 from the seismic wavefield recorded at the Earth surface, and to incorporate FGA into a seismic imaging scheme in the fashion of reverse-time migration (Etgen et al., 2009). In the next section, we test the accuracy of the approximation itself by modeling a Green's function (wave propagation from a point source) in a synthetic velocity model.

NUMERICAL TEST

We test the performance of FGA using a smoothed Marmousi model (Versteeg, 1994) shown in Figure 1. Our goal is to extrapolate the expanding wavefield from a point source from the initial condition shown in Figure 2 through 0.25 seconds in time. The reference calculation for comparison is performed with the highly accurate lowrank symbol approximation method (Fomel et al., 2013).

For the initial beam decomposition, we set the value of ε by the ratio of ℓ^2 norms of the initial wavefield f_0^ε and the wave speed f_1^ε. We adopt a fourth-order Runge-Kutta method as the numerical integrator for time propagation.

The results in Figure 3 are produced by $N = 48$, 521, and 5650 frozen Gaussian beams, which corresponds to keeping (q,p) pairs with N-largest amplitudes of $\psi_\pm^\varepsilon$. The time step is taken as 0.001 s. In the initial wavefield decomposition, the mesh sizes for q and p are 0.08 km $\times$ 0.06 km and 0.0898 km^{-1} $\times$ 0.0898 km^{-1} respectively, and the mesh size for y is 0.004 km $\times$ 0.004 km. The images are reconstructed using the mesh size 0.004 km $\times$ 0.004 km. The result in Figure 4 uses only 6 beams for the extrapolation. It is easy to see that the individual beam width remains "frozen" and does not change with position.

Comparing the results in Figure 3 with the reference wavefield shown in Figure 5(a), we can see that propagating only $N = 521$ Gaussians is sufficient to produce a qualitatively accurate result, while $N = 5650$ Gaussians produce a quantitatively accurate result by adjusting amplitudes and generating small-scale wavefield features including caustics. The difference between the result in Figure 3(c) and the reference wavefield plot is plotted in Figure 5(b) at the same scale and appears to have negligible magnitude.

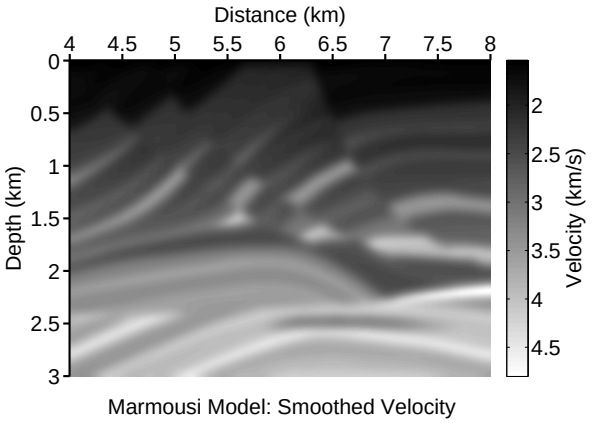

Figure 1: Smoothed Marmousi velocity model.

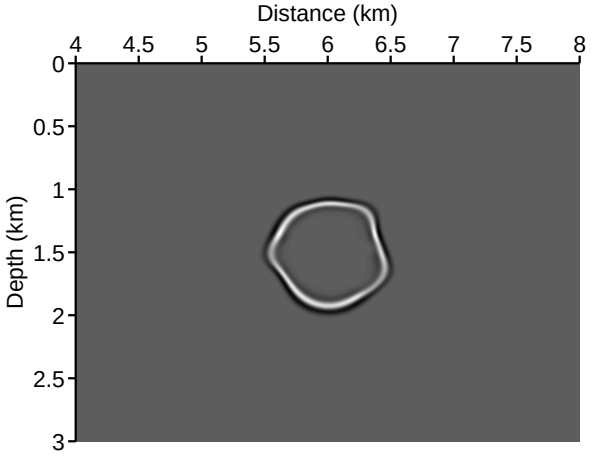

Figure 2: Initial seismic wavefield generated by a point source in the center of the Marmousi model.

CONCLUSIONS

The Frozen Gaussian Approximation (FGA) provides a stable and efficient computational tool for seismic wavefield propagation. FGA uses Gaussian functions with fixed widths, rather than those that might spread over time, as in the classic Gaussian beam approximation. As a result, a stable behavior and a good approximation accuracy can be achieved without tuning the width parameters. A rigorous mathematical analysis guarantees the accuracy of the FGA solution in modeling wave propagation beyond caustics. We have also introduced a local fast FBI transform algorithm that decomposes the initial wavefield into a set of Gaussian functions. We have numerically tested the performance of FGA using a smoothed Marmousi model. The method may find direct applications in seismic modeling and seismic imaging by beam migration.

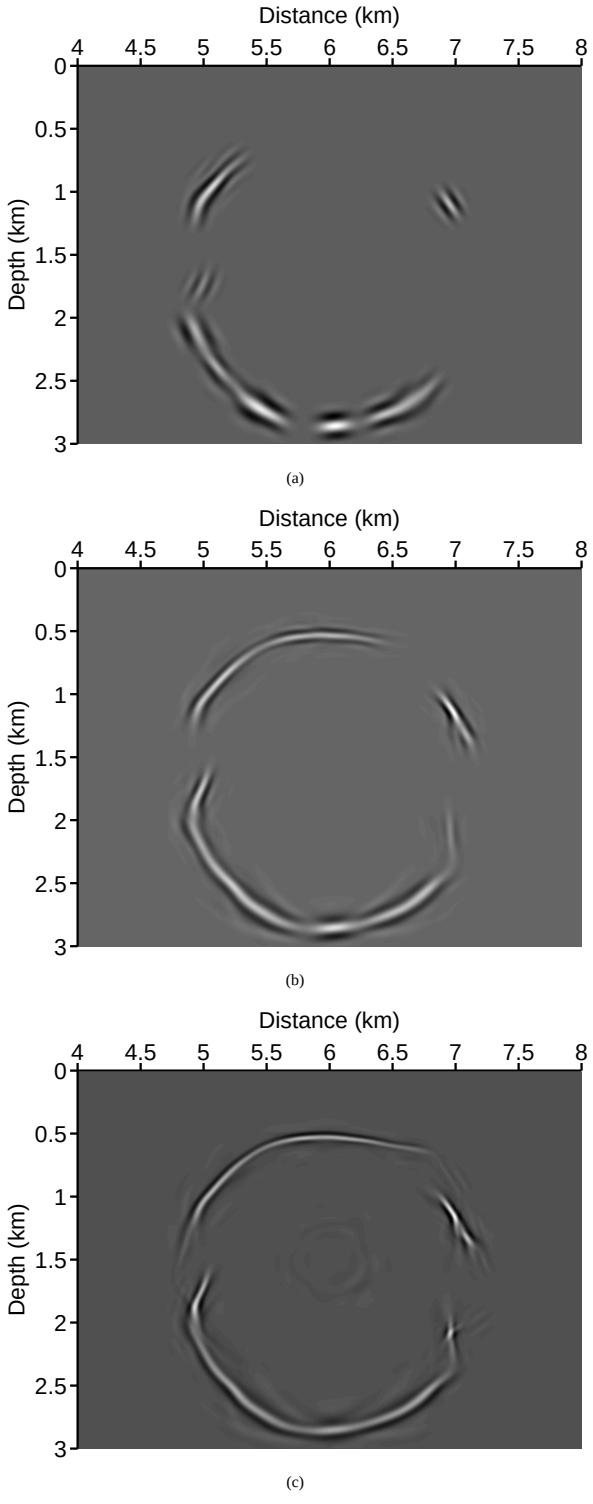

Figure 3: Wavefield predicted by FGA using (a) $N = 48$, (b) $N = 521$, and (c) $N = 5650$ Gaussians for each wave branch. The accuracy of the approximation gets improved by adding more beams.

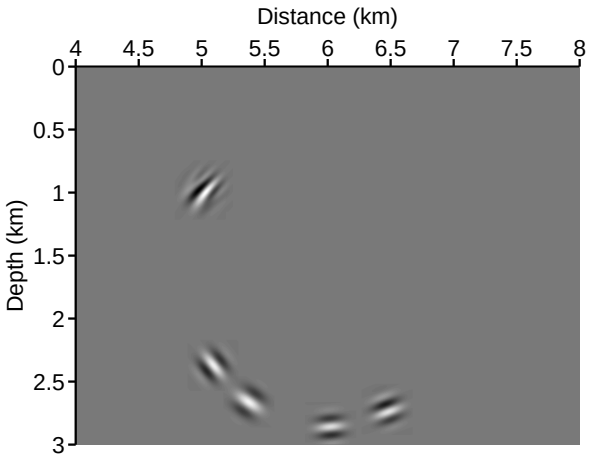

Figure 4: Wavefield at 0.25 s after the initial wavefield from Figure 2, as predicted by FGA using only six initial Gaussians for each wave branch ($N = 6$ in equation 4).

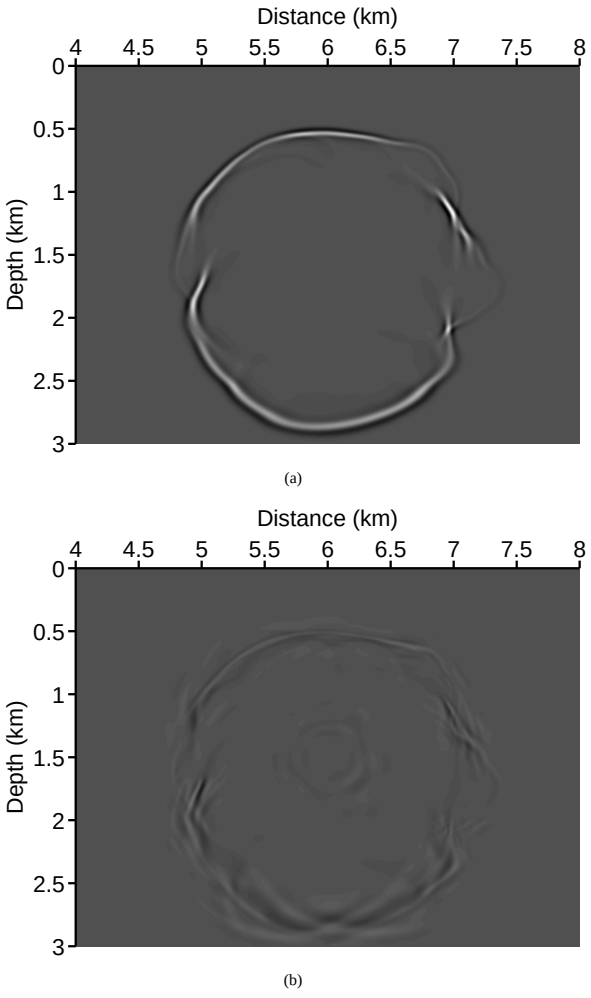

Figure 5: (a) Reference wavefield. (a) Quantitative difference between with the result in Figure 3(c)

REFERENCES

Albertin, U., D. Yingst, and H. Jaramillo, 2001, Comparing common-offset Maslov, Gaussian beam, and coherent state migrations: 71st Ann. Internat. Mtg, Soc. of Expl. Geophys., 913–916.

Bastiaans, M. J., 1980, Gabors expansion of a signal into Gaussian elementary signals: Proc. IEEE, **68**, 538–539.

Bleistein, N., and S. H. Gray, 2010, Amplitude calculations for 3d gaussian beam migration using complex-valued traveltimes: Inverse Problems, **26**, 085017.

Cerveny, V., 2001, Seismic ray theory: Cambridge University Press.

Cerveny, V., M. M. Popov, and I. Psencik, 1982, Computation of wave fields in inhomogeneous media – Gaussian beam approach: Geophys. J. Roy. Astr. Soc., **70**, 109–128.

Engquist, B., and O. Runborg, 2003, Computational high frequency wave propagation: Acta Numer., **12**, 181–266.

Etgen, J., S. H. Gray, and Y. Zhang, 2009, An overview of depth imaging in exploration geophysics: Geophysics, **74**, WCA5–WCA17.

Folland, G. B., 1989, Harmonic analysis in phase space: Princeton University Press. Annals of Mathematics Studies, no. 122.

Fomel, S., and N. Tanushev, 2009, Time-domain seismic imaging using beams: 79th Ann. Internat. Mtg, Soc. of Expl. Geophys., 2747–2752.

Fomel, S., L. Ying, and X. Song, 2013, Seismic wave extrapolation using lowrank symbol approximatio: Geophysical Prospecting.

Foster, D., R. Wu, and C. Mosher, 2002, Coherent-state solutions of the wave equation: 72nd Ann. Internat. Mtg, Soc. of Expl. Geophys., 1348–1351.

Gabor, D., 1946, Theory of communication: Proc. Inst. Electr. Eng., **93**, 429–457.

Gray, S., and N. Bleistein, 2009, True-amplitude gaussian-beam migration: Geophysics, **74**, S11–S23.

Gray, S. H., 1986, Efficient traveltime calculations for Kirchhoff migration: Geophysics, **51**, 1685–1688.

———, 2005, Gaussian beam migration of common-shot records: Geophysics, **70**, S71–S77.

Helstrom, C. W., 1966, An expansion of a signal in Gaussian elementary signals: IEEE Trans. Inform. Theory, **IT-12**, 81–82.

Herman, M. F., and E. Kluk, 1984, A semiclassical justification for the use of non-spreading wavepackets in dynamics calculations: Chem. Phys., **91**, 27–34.

Hill, N. R., 1990, Gaussian beam migration: Geophysics, **55**, 1416–1428.

———, 2001, Prestack Gaussian-beam depth migration: Geophysics, **66**, 1240–1250.

Kay, K., 1994, Integral expressions for the semi-classical time-dependent propagator: J. Chem. Phys., **100**, 4377–4392.

———, 2006, The Herman-Kluk approximation: Derivation and semiclassical corrections: Chem. Phys., **322**, 3–12.

Keho, T. H., and W. B. Beydoun, 1988, Paraxial ray Kirchhoff migration: Geophysics, **53**, 1540–1546.

Lu, J., and X. Yang, 2011, Frozen Gaussian approximation for high frequency wave propagation: Commun. Math. Sci., **9**, 663–683.

———, 2012a, Convergence of frozen Gaussian approximation for high frequency wave propagation: Comm. Pure Appl. Math., **65**, 759–789.

———, 2012b, Frozen Gaussian approximation for general linear strictly hyperbolic systems: Formulation and Eulerian methods: Multiscale Model. Simul., **10**, 451–472.

Ma, Y., and G. Margrave, 2008, Seismic depth imaging with the gabor transform: Geophysics, **73**, S91–S97.

Martinez, A., 2002, An introduction to semiclassical and microlocal analysis: Springer-Verlag.

Nowack, R., M. Sen, and P. Stoffa, 2003, Gaussian beam migration for sparse common-shot and common-receiver data: 73rd Ann. Internat. Mtg., Soc. of Expl. Geophys., 1114–1117.

Popov, M. M., 2002, Ray theory and Gaussian beam method for geophysicists: EDUFBA.

Popov, M. M., N. M. Semtchenok, P. M. Popov, and A. R. Verdel, 2010, Depth migration by the Gaussian beam summation method: Geophysics, **75**, S81–S93.

Qian, J., and L. Ying, 2010, Fast multiscale Gaussian wavepacket transforms and multiscale Gaussian beams for the wave equation: Multiscale Model. Simul., **8**, 1803–1837.

Tanushev, N. M., R. Tsai, S. Fomel, and B. Engquist, 2011, Gaussian beam decomposition for seismic migration. (ICES Report: 11-08).

Versteeg, R., 1994, The Marmousi experience: Velocity model determination on a synthetic complex data set: The Leading Edge, **13**, 927–936.